https://doi.org/10.48048/tis.2024.8718

A Novel's Evidence of MSG-Induced Craniofacial Defects in Chick Embryo Models

Suriyan Pintarasri[1], Manutsanun Santiparadon[1], Anusara Kamnate[1], Chonnapat Naktubtim[2,3], Thidarat Koomsang[2,3] and Witchuda Payuhakrit[2,3,*]

[1]Anatomy Division, Faculty of Medicine, Princess of Naradhiwas University, Narathiwat 96000, Thailand
[2]Department of Pathobiology, Faculty of Science, Mahidol University, Bangkok 10400, Thailand
[3]Pathobiology Information and Learning Center, Department of Pathobiology, Faculty of Science, Mahidol University, Bangkok 10400, Thailand

([*]Corresponding author's e-mail: witchuda.pay@mahidol.ac.th)

Received: 19 July 2024, Revised: 19 August 2024, Accepted: 22 August 2024, Published: 20 October 2024

Abstract

Monosodium glutamate (MSG), commonly used as an additive food enhancer, has been reported to have teratogenic effects on the embryo during development. The present study aimed to investigate the effect of MSG-induced teratogenicity, focusing on craniofacial formation in the chick embryo model. One hundred eighty fertilized eggs were divided into control and MSG groups. The chemicals were administered, and the results were investigated in 3-day-old embryos (ED-3), ED-6, and ED-10. The morphology and histology of craniofacial structures were studied using a stereomicroscope and light microscopy. The neural crest cells (NCCs) were investigated by the immunostaining technique. The results showed that a dose of 3 mg of MSG induced anterior neuropore opening and eye malformation in ED-3, and this was clearly demonstrated in ED-6. MSG also caused craniofacial bone malformation and delayed calcification in ED-10. Moreover, MSG induced apoptosis of NCCs and reduced the proliferation of NCCs in the craniofacial structures. These findings are the 1st report to demonstrate the teratogenicity of high doses of MSG-induced craniofacial defects in chick embryos during organogenesis.

Keywords: Monosodium glutamate, Craniofacial defect, Neural crest cells, Chick embryo, Teratogen

Introduction

Craniofacial development in the vertebrate embryo, including humans, occurs at the end of the 4th and 10th weeks [1]. The formation is an enormously complex, multi-step process that is regulated on a genomic, molecular, cellular, and tissue level [2]. In the early stages of craniofacial development, which rely on the growth and fusion of 5 facial primordia: The frontonasal prominence (FNP), pairs of branchial arches, maxillary processes, and mandibular processes [1,3]. During this process, the FNP is rapidly outgrowing and divided into lateral and medial nasal prominences, which will give rise to the forehead and nose in the future. The maxillary processes fuse to the FNP and give rise to the upper jaw, while the mandibular processes fuse in the midline and give rise to the lower jaw.

In addition, the driving force behind each process of growth and fusion is the formation of neural crest cells (NCCs), especially in the cranial NCCs. The NCC's functions - specification, emigration and migration, proliferation, survival, and ultimate fate determination - play a crucial role in regulating craniofacial development [4]. The cells migrating rostrally toward the most anterior part of the brain vesicle in development establish the FNP. According to the craniofacial bone ossification study, 5 facial primordia united by neural crest mesenchyme were followed by both intramembranous and intracartilaginous ossification [5,6]. Furthermore, the signaling molecules named Wnt, bone morphogenetic protein (Bmp), fibroblast growth factor (Fgf), and Sonic hedgehog (Shh), which are the four common signaling molecules that are expressed and controlled by NCCs, can also be the key to providing positional cues and regulating growth and differentiation drivers during craniofacial development [3,7].

In addition, the craniofacial structures, including the eye and ear, develop along with the other craniofacial structures. In the eye, development begins at the 6th week of development with the lateral outgrowths of FNP, which form a double-layered structure called the optic cup. The inner layer is derived from the neural retina, while the outer layer is derived from the retinal pigmented epithelium. Furthermore, the mesenchymal cells that migrate into the space between the surface epithelium and the developed corneal endothelium to form the future corneal stroma derive from the NCCs [8]. Whereas ear development occurs at the 4th week of development by the ectodermal invagination to form an otic pit (OP) around the hindbrain. The sides of the OP fuse to form a hollow piriform structure lined, like a teardrop, with columnar epithelium, called the otic vesicle (OV). The OV forms 2 components, including a ventral saccular portion, which is involved in hearing, and a dorsal utricular portion, which is a balance system [9]. In addition, the NCCs from the rhombomere region also contribute to the sense organs in the inner, middle, and outer ear. The failure of craniofacial prominence and pharyngeal arch formation results in craniofacial defects (CFDs), such as cleft lip and/or palate, craniosynostosis, encephalocele, hemifacial microsomia, anophthalmia, external ear deformities, etc. [7,10], which are well established, however, the other causes need to be further investigated.

Craniofacial defects (CFDs) are a group of birth defects with an incidence rate of approximately 1 in 600 births [11]. These defects lead to problems with medical care, lifetime burden, and financial support [12]. The etiology of CFDs is multifactorial, including genetics or environmental factors (drugs, teratogens, etc.). Most of the causes are unknown, and the mechanism is still unclear. Previous studies have primarily focused on the etiology of genetics in the pathogenesis of CFDs, while a few studies have focused on the environmental factors that induce CFDs. Meanwhile, some studies have revealed chemical-induced craniofacial anomalies in a zebrafish model [13].

The CFDs are strongly associated with neural crest cell (NCC) development, with defects in the formation, migration, and differentiation during embryogenesis [14,15]. NCCs are a transient group of embryonic cells known as ectomesenchyme, which play an essential role in embryogenesis. The cells arise from the neural tube border and can be classified as cranial, cardiac, vagal, or trunco-sacral regions [16,17]. A variety of cell types in craniofacial structures such as bone, cartilage, parts of organs of special senses such as the ear and eye, and neuronal cells are produced exclusively by cranial NCCs and a portion of cardiac NCCs [18-22]. The abnormality of NCC functions during craniofacial development leads to CFDs,

for example, exencephaly or maxillofacial defects [23,24]. Many factors that cause NCC dysfunction may be caused by the gain or loss of function, such as genetics, environmental factors, etc. As reported in previous studies, the teratogen is one of the causative agents of NCC fatalities [25,26].

Monosodium glutamate (MSG) is a glutamic acid in one sodium form. It is an additive in foods to enhance the Umami flavor [27]. The dietary MSG was mainly metabolized and absorbed along the intestinal tract, and its crucial physiological role in neuronal function as a neurotransmitter was observed [28]. However, MSG has been reported to have adverse effects on humans after consuming a high dose of more than 3 g of MSG per day, including metabolic disorders and neurotoxicity [29-33]. Surprisingly, a few reports used animal studies as models for pregnant women to study the adverse effects of MSG consumption. Moreover, there is no evidence that maternal consumption of MSG causes birth defects in infants. Nevertheless, high doses of MSG might induce craniofacial defects in the fetus. Recently, we reported MSG-induced BDFs in ED-3 chick embryos by observing effects in various organs [34]. In this study, we aim to investigate MSG-induced CFDs.

Chick embryos are amniotic models that have been extensively used in biomedical research, not only in genetic observation but also in chemical screening studies, because they have significant similarities to human embryos at the molecular, cellular, and morphological levels [35-38]. Hamburger and Hamilton (1951) described the chick embryo in each developmental stage, known as the "HH stage". O'Rahilly reported the fundamentals of studying human development in the Carnegie stage (CS). In humans, ED-33, ED-48, and ED-58 (at 2 months of pregnancy) were similar to ED-3, ED-6, and ED-10 in chick development, respectively [39]. Furthermore, the chicken skull can be used as a human skull model because the skull vault is composed of cranial bones named frontal, parietal, and occipital, while facial bones are called nasal, pterygoid, maxilla, palatine sphenoid, and mandible [40]. Although the chick embryo provides excellent opportunities for screening for birth defects, there are few reports on the adverse effects of MSG-induced teratogenicity that used chick embryo studies [31,32,41]. In addition, there are no studies on the effects of MSG-inducing craniofacial defects in chick embryo models. Therefore, the present study aims to investigate the mechanism of MSG-induced CFDs in ED-3, ED-6, and ED-10 of chick embryo development to understand the mechanism and further apply in teratogenicity studies and treatment during organogenesis.

Materials and methods

Chemicals and antibodies.

Monosodium glutamate (MSG) was purchased from Sigma - Aldrich (USA). The 3 mg of MSG was prepared by dissolving 0.0359 g of MSG powder into 10 mL of warm, sterile, normal saline solution (NSS). Anti-HNK-1 antibodies were purchased from Sigma-Aldrich (C6680, USA), and secondary antibody conjugated-HRP was purchased from Merck Millipore (AP124P, USA). Anti-Caspase-3 (ab32351, Rabbit monoclonal) was purchased from Abcam and anti-BrdU (Mouse mAb #5292, Mouse monoclonal), was purchased from Cell Signaling Technology, while fluorescein-conjugated secondary antibodies Goat Anti-Rabbit IgG (Alexa Fluor® 488, ab150077) and Goat Anti-Mouse IgG (Alexa Fluor® 594, ab150116) were also purchased from Abcam.

Chick embryo experiments

The freshly laid, fertilized, Rhode Thai eggs (*Gallus domesticus*) were obtained from the Baan Rai hatchery, an affiliated company of CP, Ban Phru sub-district, Hatyai district, Songkhla province, Thailand (6°53'39.2"N 100°27'50.1"E). The study was approved by Walailak University Intuition Animal Care and Use Committee (WU-ACUC-65029). Although chick embryos younger than 12 days are exempt from animal ethics approval [42], we remain fully committed to ensuring their welfare throughout the experiment. The 180 fertilized eggs were cleaned with sterile water, then weighed, and incubated at 37 ± 0.5 °C with 70 - 80 % humidity in a humidified incubator and automatically turned 120 degrees 3 times per day. The experiments delivered a single injection of 50 µL soluble agent concentration of 3 mg/kg egg weight (LC50 = 3.84 mg/kg), into the fertilized eggs after 21 h of incubation using the ovo-injection method [31]. One hundred and eighty fertilized eggs whose average weight was 0.62 ± 0.37 kg were divided into 2 groups, as shown in **Figure 1**. The diagram shows the study period, the number of subjects, and the chemical agent injected into each group. The aim of using the ED-3 (n = 60), and ED-6 (n = 60) was to study the morphology, and histology. Meanwhile, the aim of using the ED-10 (n = 60) was to study the morphology and calcification of craniofacial bone.

The morphological study

The whole bodies of 3-day-old embryos (ED-3; HH4) in each group were stained with Mayer's Carmine for 30 min, dehydrated with a graded series of alcohol for 20 min for each change, cleared with xylene for 30 min, mounted by using Canada balsam (Panreac, Spain), and then observed under a stereomicroscope (Leica EZ4 W, Germany) and photographed. In addition, the whole bodies of 6- (ED-6; HH36) and 10-day-old embryos (ED-10; HH36) were photographed, and the eye diameter, beak length, and bone ratio were measured and analyzed using the Fiji program.

The histological study

The ED-3 was fixed with 4 % paraformaldehyde in PBS, processed, and embedded in paraffin wax. The paraffin block was sectioned at 4 - 6 µM. The tissue sections of each group were stained with hematoxylin and eosin (H & E), observed under a light microscope (Olympus BX53, Japan), and photographed.

Immunohistochemistry staining

To investigate the NCCs on 3-day-old embryos (ED-3), sections of paraffin-embedded on the ED-3 tissue were dewaxed, rehydrated, and retrieved using 10-mM sodium citrate buffer (pH 6.0) for 20 min. Sections were then rinsed in PBS, and a protein blocker (Vector, USA) was applied to block nonspecific background staining for 5 min. Sections were incubated with the anti-HNK-1 (1:100), a specific marker of NCCs, at 4 °C overnight. The slides were washed with PBS, followed by incubation with the secondary HRP-conjugated antibody (1:500) for 4 h. The slides were then washed in PBS, followed by incubation with DAB Substrate (Vector, USA) for 20 min at room temperature and then counterstained in Mayer's

hematoxylin for 30 s. The slides were observed under a light microscope (Olympus BX53, Japan), photographed, and measured for their mean IHC intensity using the Fiji program.

Immunofluorescence staining

The apoptosis and proliferation of NCCs were determined using the colocalization of HNK-1 and caspase-3, and the colocalization of HNK-1 and BrdU, respectively, on 3-day-old embryos. Briefly, tissue sections of paraffin were dewaxed, rehydrated, and retrieved using a 10-mM sodium citrate buffer (pH 6.0) for 20 min. Subsequently, the tissues were permeabilized with 0.1 % Triton X-100 for 10 min at room temperature, washed 3 times with PBS, blocked with PBS containing 5 % bovine serum albumin for 1 h, and incubated with primary antibodies against HNK-1 (1:100), caspase 3 (1:100) and BrdU (1:200) overnight at 4 °C in a humidified chamber. The slides were washed with PBS, followed by incubation with the fluorescein-conjugated secondary antibodies (1:500) for 30 min. DAPI was used for counterstaining. The slides were washed with PBS and mounted using 50 % glycerin in PBS. The slides were visualized by a fluorescence microscope equipped with a camera (Eclipse Ni-U, Nikon), photographed, and measured for their mean fluorescence intensity using the Fiji program.

The cartilages and bones study

The craniofacial cartilage and bone formation were studied on ED-10. The whole embryo without internal organs was stained with Alcian blue and Alizarin Red staining. The embryo was cleared of the skin and soft tissue by soaking it in a mixture of 10 % KOH and H_2O_2 (ratio 1:9) until the specimen was clear and transparent. Then the specimen was washed in distilled water for several days before being stained with Alcian blue for 2 days. Grading alcohols of 95, 75, 40 and 15 % and distilled water were used to wash the dye for 3 h in each change, after which the specimen was transferred to saturated Alizarin Red S solution, and the staining was stopped after the bones were distinctly red. The specimen was transferred through a 0.5 % KOH-glycerin series in the following ratios: 3:1, 1:1, and 1:3 to pure glycerin, 1 day for each step. The cartilage and calcified bones were observed under a stereomicroscope (Leica EZ4 W, Germany) and photographed. The percentage of calcification ratio was determined and modified from the method previously described by the Fiji program [43].

Statistical analysis

The sample size was calculated by Statsols, a provider of n-Query Advisor, based on eye diameter estimation in ED6, and the number in each group is 30. The data were analyzed using Prism software version 8. All data were expressed as the mean ± SD. Differences in the measured parameters in the different studied groups were tested using the One-Way ANOVA followed by post-hoc Tukey HSD (Honestly Significant Difference) test and significance was considered at $p < 0.05$.

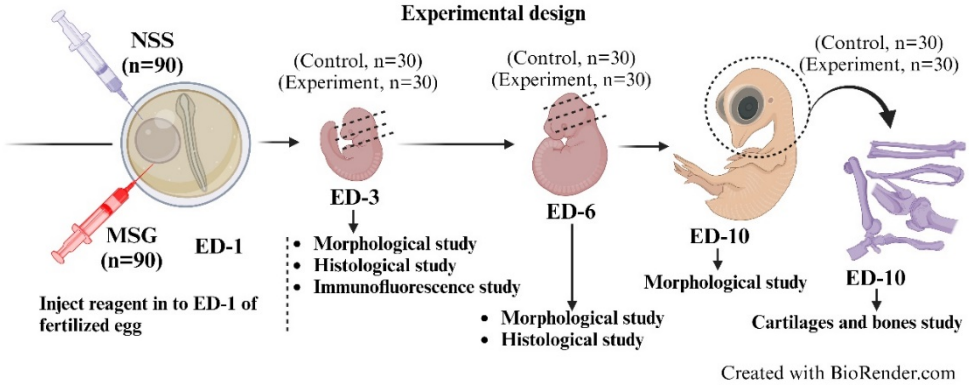

Figure 1 The schismatic diagram of the experimental design shows the details of the experiments. The diagram shows the period of study, the number of subjects, and the chemical agent that was injected into each group. The aims of 3-day-old embryos (ED-3) and ED-6 were to study the morphology and histology while the aim of ED-10 was to study the calcification of craniofacial bone. Created with BioRender.com, MSG = Monosodium glutamate, NSS = Normal saline solution.

Results and discussion

MSG-induced anterior neuropore opening and eye malformation in 3-day-old embryos.

We explored the effects of MSG on craniofacial malformation. The results showed that MSG induced teratogenicity by delaying growth and organ malformation in the head and face. The embryo from the 3 mg MSG group showed an anterior neuropore opened, as indicated by the black arrows (D). The few BA appearances which indicated by asterisk symbol (F). At the same time, there was also brain vesicle narrowing and eye malformation, as shown in photo F. In the MSG group, the developmental disruptions were explored by the smallest head, anterior neuropore opening, few of branchial arch formation, and anophthalmia (**Figures 2(D)** to **2(F)**). The tissue sections from the MSG groups with 3 mg of MSG confirmed the effects of MSG on brain vesicles, branchial arch, and eyes by revealing the anterior neuropore opening (20.00 %, $p < 0.05$), a few of branchial arch formation (20.00 %, $p < 0.05$), and eye malformation (6.67 %, $p < 0.05$) when compared with the control (**Figures 2(A)** to **2(C)**). These results indicate that MSG-induced anterior neuropore opening and a few branchial arch and eye malformations result in craniofacial malformations.

MSG-induced NCC apoptosis and -reduced NCCs proliferation in 3-day-old embryos.

As the MSG affected craniofacial defects in ED-3, we further investigated the NCCs that might be associated with craniofacial defects. Therefore, the NCCs were localized by using the HNK-1 marker (**Figures 2(I)** to **2(S)**), and the mean IHC intensity was determined (**Figures 2(L), 2(P)** and **2(T)**). We observed that the tissue sections through the cranial and facial region in the control group had a high NCC subpopulation, which was well-localized on the frontonasal prominence (FNP), a part of the brain vesicles (BV), ears, and eyes. In contrast, the MSG group had a significantly decreased NCC population, as observed by a few remaining NCC populations in the eyes ($p<0.01$), ears ($p<0.0001$), and FNP ($p<0.001$) when compared with the control.

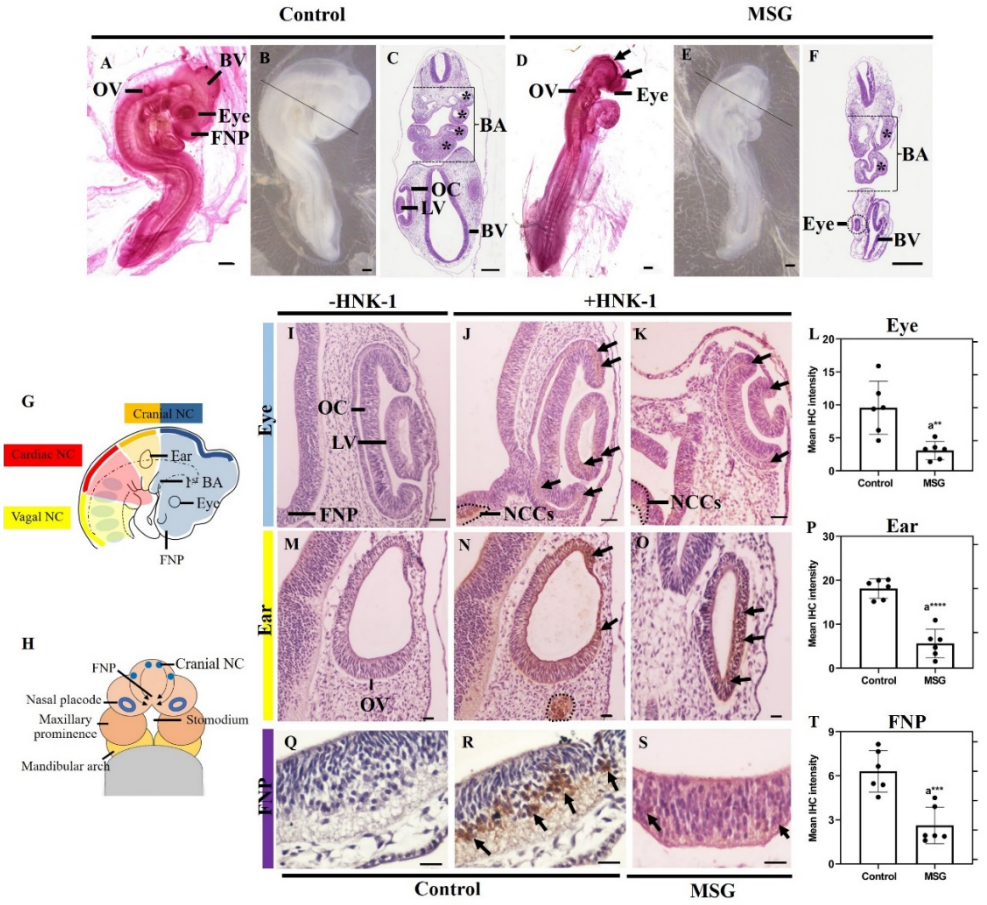

Figure 2 Photographs showing the whole body of a surviving ED-3 in the dextro-dorsal view ((A), (B), (D) and (E)). The pictures include Mayer camalum staining ((A) and (D)), the whole embryo without staining that indicates the section through the head with a black straight line ((B) and (E)), and the micrograph tissue sectioning stained with H & E ((C) and (F)). OV = otic vesicle, BV= brain vesicle, FNP = frontonasal prominence, OC = optic cup, LV = lens vesicle, and BA = branchial arches. Following photographs in (G) is the diagram of the NCCs' origin and migratory route in the craniofacial region, while (H) is a rostral view showing structures that will give rise to the face, including the FNP, nasal placode, maxillary prominence, mandibular arch, and stomodaeum. The tissue sections and stains on the eye, ear, and FNP with anti-HNK-1 by IHC technique on ((I), (M) and (Q)) showed a negative (-HNK-1) and positive (+HNK-1) on ((J), (K), (N), (O), (R) and (S)) for the control and MSG group. The tissue staining showed the population of NCCs as indicated by black arrows. In addition, the tissue among the experiment group shows different intensities of HNK-1 in the bar graph on (L), (P) and (T). The pictures (A) - (F) were captured under a light microscope at 1.25× magnification, scale bar = 500 µM, n = 30, and the pictures (I) - (K), (M) - (O) and (Q) - (S) were captured under a light microscope at 10×, scale bar = 50 µM. Data given are mean ± SD, (n = 5). Significant differences** = $p < 0.01$, *** = $p < 0.001$, **** = $p < 0.0001$; one-way ANOVA followed by post-hoc Tukey HSD test. * indicate the position of branchial arches (BA), black arrows indicate an anterior neuropore opened.

We assessed the apoptotic NCCs using caspase-3 colocalized with HNK-1 markers (**Figure 3**) and measured the mean fluorescence intensity to confirm the effect of MSG on NCCs (**Figures 3(H), 3(P)** and **3(X)**). The white arrow indicated the apoptotic NCCs, which were positive for both HNK-1 and caspase-3 staining. We observed that the tissue sections through the cranial and facial regions in the control group had high NCC signaling with low caspase-3 intensity on the eyes, ears, and FNP (**Figures 3(A)** to **3(C)**, **3(I)** to **3(K)** and **3(Q)** to **3(S)**). Conversely, the MSG group had a decreased NCC population as observed by a few NCC signals on the eyes, ears, and FNP when compared with the control and had a significantly higher intensity of apoptotic NCCs in the eyes ($p < 0.0001$), ears ($p < 0.0001$), and FNP ($p < 0.0001$) when compared with the control (**Figures 3(F)**, **3(N)** and **3(V)**). Moreover, the anterior neuropore opening was observed in the eye section, indicating a white broken line in the HNK-1 stain.

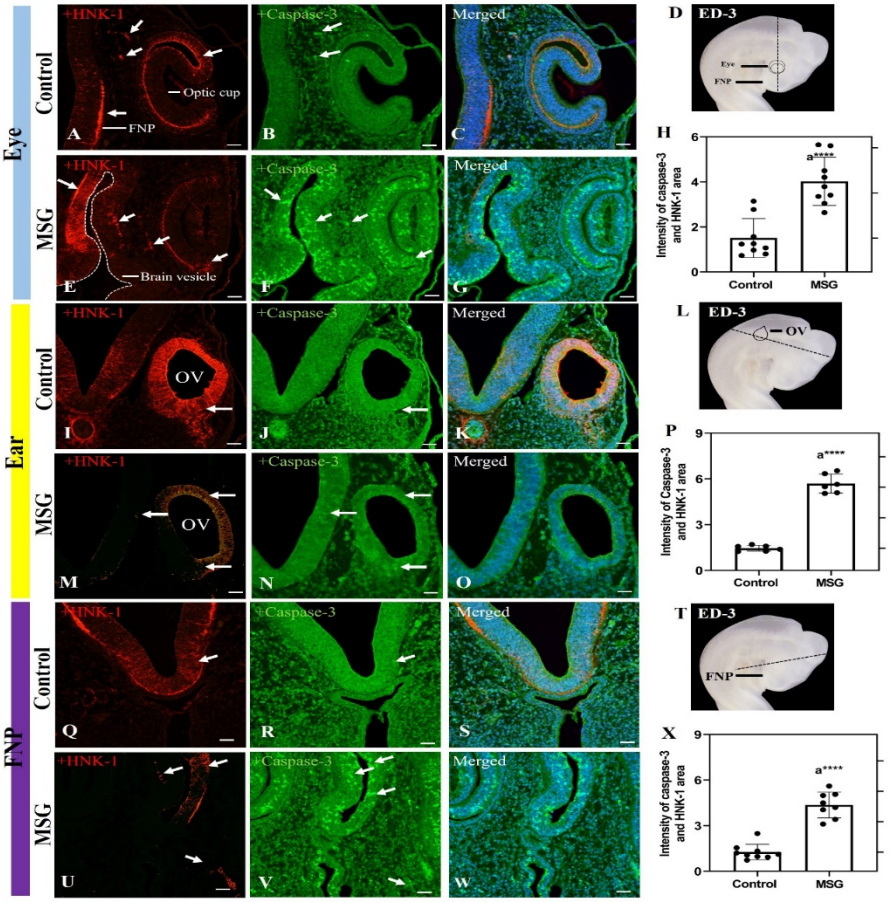

Figure 3 The photographs show the tissue sections and fluorescent labeling with anti-HNK-1 and anti-caspase-3 that were used to count the apoptotic NCCs on the ear, eye, frontonasal prominence (FNP), and brain vesicle (BV). A red signal indicates the NCCs, while the apoptotic cells are presented in green. In addition, the whole embryo without staining indicates the section through the eye, ear, FNP, and BV with a black straight line on (D), (L), and (T), while the tissue of the experiment group shows different intensities of HNK-1 and caspase-3 in the bar graph on (H), (P), and (X). The pictures were captured under a fluorescence microscope at 20× magnification, with a scale bar = 50 µM. Data given are mean ± SD, (n = 5). Significant differences **** = $p < 0.0001$; one-way ANOVA followed by post-hoc Tukey HSD test.

Furthermore, we assessed the NC cell proliferation using BrdU colocalized with HNK-1 markers (**Figure 4**). NC cell proliferation was identified and determined based on mitotically active and expressed BrdU [43]. The intensity of the BrdU and HNK-1 area was determined and represented from the total area on the eye, ear, and FNP from the control and MSG group (**Figures 4(J) - 4(L)**). Compared with the high number of proliferative NC cells demonstrated in the control group, the MSG-treated group had significantly decreased NC cell proliferation, as observed by the small number of proliferating NC cells in the eyes ($p < 0.001$), ears ($p < 0.0001$) and FNP ($p < 0.0001$) when compared with the control group.

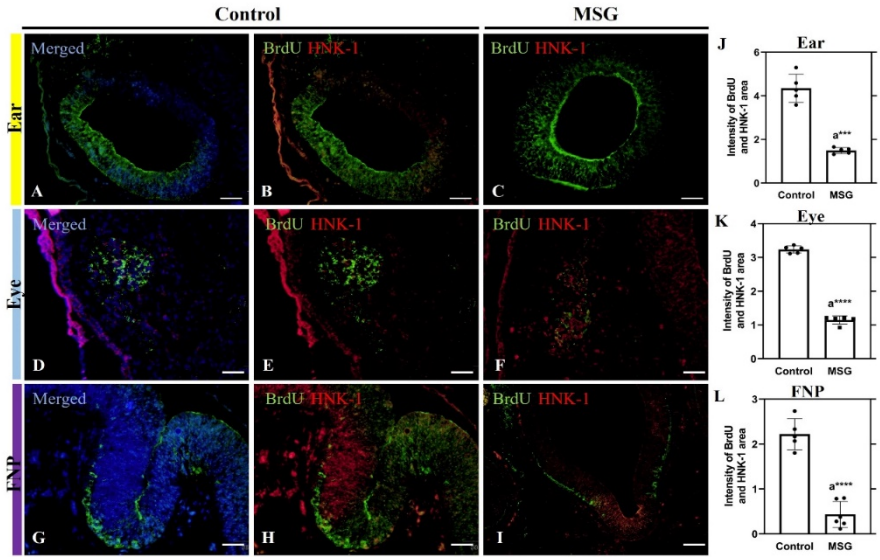

Figure 4 The photograph shows the tissue sections and fluorescence labeling with BrdU-colocalized with anti-HNK-1 used to count the proliferative NCCs on the eye, ear, and frontonasal prominence (FNP). NC cell proliferation was identified and determined based on BrdU and HNK-1 expressed cells (green and red colors respectively). Bar graphs (J), (K) and (L) are the intensity of the BrdU and HNK-1 area was determined and represented from the total area on the eye, ear, and FNP from the control and the MSG groups. The pictures were captured under a Fluorescence microscope at 20×, scale bar = 20 µM. Data given are mean ± SD, (n = 5). Significant differences *** = $p < 0.001$, **** = $p < 0.0001$; one-way ANOVA followed by post-hoc Tukey HSD test.

MSG-induced brain vesicle opening and microphthalmia in 6-day-old embryos.

Craniofacial malformation in ED-6 was observed in both external morphology and histology. As a result, the MSG group had an incidence of the brain (33.33 %, $p < 0.05$) and eye defects (16.67 %, $p < 0.05$) as shown in **Figures 5(D)** to **5(F)**. Furthermore, the eye diameter showed a significantly smaller size ($p < 0.05$) when compared with the control (**Figures 5(A)** to **5(C)**). The tissue sections from the MSG groups confirmed MSG-induced brain vesicle damage by showing that the anterior neuropore had opened, leading to an unfused forebrain, as seen in **Figure 5(E)**. Moreover, eye malformation was observed in **Figure 5(F)**. These results suggest that MSG causes craniofacial malformation by inducing brain vesicle damage and microphthalmia in 6-day-old embryos, which supports the findings in ED-3.

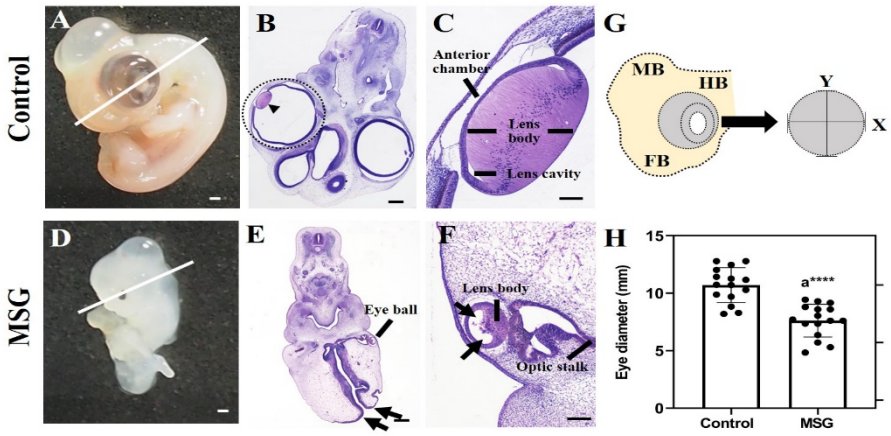

Figure 5 Photographs of ((A) and (D)) showing the whole body of ED-6, and tissue sectioning with H & E staining ((B) - (C) and (E) - (F)). Normal embryos from the control group showed brain vesicles and a vesicular eye composed of a lens in the anterior aspect. The tissue section demonstrated an equal lens body indicated by blackhead arrow ((B) and (C)). The MSG group showed brain vesicles opened indicated by black arrow with microphthalmia (E). The pictures were captured under a stereomicroscope and light microscope, scale bar = 500 µM. Photographs of (G) is the drawing picture demonstrates the BV; forebrain (FB), midbrain (MB), and hindbrain (HB) and the eye measurement procedure on both the X and Y axis. Photographs of (H) is the bar graphs demonstrate the eye diameter compared to the control and MSG groups. Data represent mean ± SD, (n = 30). Significant differences **** = $p < 0.0001$; one-way ANOVA followed by post-hoc Tukey HSD test.

MSG-induced beak defects, brain herniation, and eye defects in 10-day-old embryos.

As in ED-10, the MSG group had a significantly increased percentage of beak, brain, and eye defects at 20.00 ($p < 0.05$), 20.00 ($p < 0.05$) and 6.7 ($p < 0.05$) %, respectively, when compared with the control (**Table 1**). Moreover, the MSG group also showed brain tissue herniation, as indicated by the black asterisk, eye and ear defects, and beak deformity (**Figures 6(B)** to **6(D)**). These results indicate that the MSG-induced teratogenicity was induced by inducing craniofacial malformation in the MSG group compared with the control.

Table 1 The frequency percentages of particular developmental defects in living ED-10 in control and experiment groups.

Types of malformation	Groups	
	Control (n = 30)	MSG (n = 30)
Beak defects	0	20.00*
Brain defects	0	20.00*
Eye defects	0	6.70*

The control groups (NSS) showed 0 % embryonic malformations. The MSG groups showed a variety of embryonic malformations compared to the control (NSS). * There was a significant difference between MSG and control (NSS), * = $p < 0.05$.

MSG-induced craniofacial bone malformation and delayed calcification.

The effects of MSG were further observed in ED-10, which provided the opportunity to investigate bone calcification. We calculated the bone calcification ratios from the Fiji program that detects the intensity of bone on the cranium and beak length in ED-10 (**Figures 6(E)** to **6(H)** and **6(I)** to **6(J)**). The 5 whole embryos in each group were stained with Alizarin Red to demonstrate calcified bone and Alcian Blue to enable observation of cartilage development (**Figures 6(E)** and **6(G)**). The results show that the control had a high density of bone and easily observed bone shape in most of the cranium and face, as shown in **Figure 6(F)**. The MSG induced teratogenicity by disturbing bone formation and calcification, leading to reduced beak length. ($p < 0.0001$), as observed in **Figure 6(I)** and reducing the calcification ratio ($p < 0.0001$), as shown in **Figure 6(J)**.

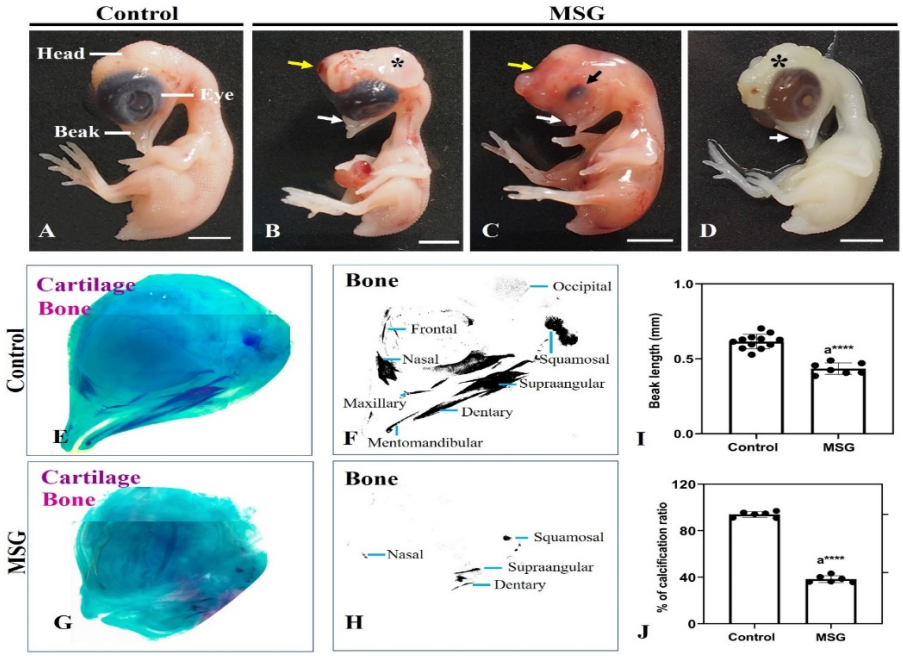

Figure 6 Photographs showing the whole body of the surviving ED-10 from the control and experimental groups in the lateral view (A) - (D). Focusing on the craniofacial structures, the normal embryo can be identified in (A) as follows: Beak, eyes, and head. The defects on the head in (B) and (C) are brain tissue herniation (black asterisk), beak deformity in (B) - (D), white arrow; eye absence in (C), black arrow; and hematoma in (B) and (C), yellow arrow. In addition, photographs in (E) and (G) show a lateral view of the ED-10 skull, stained with Alizarin red and Alcian blue. The calcified bone showed up in red, while the blue was cartilage. In control, cranial bones (including frontal, occipital, and squamosal bones), facial bones (nasal), and jaw bones (maxillary, mentomandibular, dentary, and supraangular) were well developed (F) and the remaining bones showed in H. The bar graphs demonstrate jaw bone development observed by beak length (I). The bar graphs represent the percentage of calcification ratio calculated by the intensity from the Fiji program as 100 % of the control (J). The pictures were captured with a digital camera; scale bar = 0.5 mm. The data represent mean ± SD, (n = 30). Significant differences **** = $p < 0.0001$; one-way ANOVA followed by post-hoc Tukey HSD test.

MSG is widely used as a flavor enhancer. Although it does not cause much toxicity in adults, the teratogenicity it induces in embryonic development during the prenatal period is still controversial. We first demonstrated the teratogenicity of MSG in the chick embryo model in ED-3, ED-6, and ED-10, which is comparable with the first 2 months of pregnancy in humans. In the present study, we apply a single dose of 3 mg of MSG, followed by a previous report [34]. The 3 mg of MSG can induce craniofacial defects in the chick embryo model. The 3 distinct study periods (ED-3, ED-6, and ED-10) were chosen based on their relative importance as follows: 1) ED-3 (HH18) is a critical period for studying NCC functions during craniofacial development. Since NCCs have a transient lifespan during development, extending only to ED-4 (HH22), they give rise to various specialized cell types or tissues. 2) ED-6 (HH28) is suitable for observing the development of facial structures and organs such as the eyes, ears, and brain tissue, as this period marks the continuation of organogenesis, which persists from day 6 until the egg hatches (HH46). 3) ED-10 (HH36) is primarily used to study cartilage and bone formation, as chondrification and ossification processes occur during the HH36 stage, making it a critical period for the present study.

The negative effect of MSG follows an all-or-none theory. When embryos are exposed to MSG at either high or low concentrations during organogenesis, and depending on the duration of exposure, the embryonic cells are unable to mitigate its toxic effects. This results in immediate and irreversible abnormalities, leading to developmental retardation or embryonic death. Consequently, the present study observed NCC-associated craniofacial defects on ED-3, ED-6, and ED-10. Our findings demonstrated MSG-induced anterior neuropore opening, eye and branchial arch malformation in 3-day-old embryos, which was clearly demonstrated in ED-6. Additionally, on day 10 of embryo development, anencephaly was associated with brain herniation, with a significantly increased prevalence of beak, brain, and eye defects in the MSG-treated group, which indicates the teratogenicity of MSG-induced craniofacial bone malformation. The few pairs of branchial arch formations led to lower beak deformities and ear defects, which were observed in ED-10. These findings were consistent with those of Adam and his colleague [44], who described the normal and abnormal embryological development of the branchial arches and the anatomical structures of the head and neck that derive from each arch. Furthermore, our findings also showed that MSG treatment significantly delayed bone calcification in craniofacial bones. The delays in ossification were correlated with bone length and bone ratio. The results are consistent with the studies from Liu *et al*. [12] and Demirtas [45] in describing the occurrence of craniofacial malformations from the induction of the chemical substance called teratogen. We found that MSG causes CFD-like alcohol exposure, which was studied by Zhang *et al.* [46] and Thomas *et al.* [47], who reported alcohol-induced craniofacial bone defects by negatively affecting cranial neural crest development and induced craniofacial growth retardation in animal embryos. On the other hand, the MSG is inattentive to limb defects, which is inconsistent with the studies from Therapontos *et al.* [48], and Kim and Scialli [49], who reported the teratogens of thalidomide, a morning sickness drug, induced limb defects. Therefore, it concludes that MSG has the ability to induce teratogenesis similar to alcohol, unlike thalidomide. These researchers reported the mechanisms of teratogen that interrupted the activities of cells during their development, such as mitosis, cellular interactions, protein synthesis, and cell migration. The disruption of cellular activity causes dysmorphogenesis.

From the previous studies have demonstrated that teratogens induce necrosis cell death in embryonic structures, especially the facial bone stem cells, also known as neural crest cells (NCCs) [12]. Our results also showed that MSG induces the destruction of NCCs in the craniofacial structures by increasing NCC apoptosis. The disturbance of MSG also causes NCC dysfunction in cell proliferation. The failure of NCCs to properly balance cell division and migration events may result in birth defects, termed neurocristopathies [50]. The low prevalence of NCCs during craniofacial development may cause cranial and facial bone malformations. This indicates that the teratogenicity of MSG was associated with the disturbed function of NCCs in craniofacial structures during organogenesis leading to craniofacial defects in chick embryos. However, further study into the mechanism of NCC defects is required to confirm the association of NCC destruction with craniofacial anomalies. Other mechanisms might be involved in MSG-induced craniofacial defects, such as oxidative stress. Previous studies revealed that zinc oxide nanoparticles initiated the production of reactive oxygen species (ROS), which subsequently caused cell toxicity, inflammation, and apoptosis. These processes resulted in the reduced production and migration of cranial neural crest cells, leading to craniofacial defects in chick embryos [51]. The MSG-treated group showed a reduction in the number of HNK-1-positive cells, but the distribution was similar to the control group. However, these findings should be further investigated regarding the function of NCCs during exposure to MSG and their compensation activity until they are fully differentiated into organs at the molecular and cellular levels.

Our study reveals MSG-induced craniofacial teratogenicity by promoting cranial and facial bone malformation in the chick embryo model. Even though there is a lack of evidence to demonstrate the effect of MSG on craniofacial defects in humans, a high concentration of MSG may cause craniofacial defects. The 3- to 10-day-old chick embryo model is an effective model for comparison with humans to describe craniofacial morphological and histological changes. This is due to the consistent patterns of growth and development, particularly in the NCC, which plays a crucial role in the formation of craniofacial structures and the development of nervous tissue in the facial region. Moreover, they share the same pattern of facial prominences such as FNP, Maxillary, and Mandibular that present during day 6 (HH29) in chickens and after week 8 in humans (CS48), as well as chondrification and ossification on day ED10 (HH36) of growth in chickens and after week 7 in humans (CS58) [42]. Therefore, using chick embryos as a model for studying embryogenesis is considered comparable to human embryonic development. Otherwise, further study is needed to clarify the mechanisms of MSG-induced teratogenicity at the cellular and molecular levels associated with the function of NCCs, and the teratogenic effects of MSG metabolites, which would provide a significant pathologic mechanism of MSG-induced teratogenicity.

Conclusions

Our findings reveal that MSG-induced teratogenicity causes CFDs in chick embryos. Moreover, the longer the exposure to MSG, the more serious the consequent effects of CFDs. The MSG also induced apoptosis of NCCs, reduced the proliferation of NCCs in the craniofacial structures, and led to birth defects (BDFs) similar to those in humans. The MSG-induced anterior neuropore opening, eye, and branchial arch malformations in ED-3 were clearly demonstrated in ED-6. Additionally, on day 10 of embryonic development, anencephaly was associated with brain herniation, beak, brain, eye defects, and craniofacial

bone malformation. Therefore, these experimental protocols benefit teratogenicity studies, and the results can be applied to future studies to elucidate the causes of BDFs during organogenesis.

Acknowledgements

We would like to thank the research staff of the Anatomy Department and Pathobiology Department for supporting each technique performed in this research. The facilities are supported by the Pathobiology Information and Learning Center, Department of Pathobiology, Faculty of Science, Mahidol University, Thailand.

References

[1] S Rinkoff and RE Adlard. *Embryology, craniofacial growth and development.* StatPearls Publishing, Treasure Island, Florida, 2022.

[2] AP Murillo-Rincón and M Kaucka. Insights into the complexity of craniofacial development from a cellular perspective. *Front. Cell Dev. Biol*. 2020; **8**, 620735.

[3] DM Roth, F Bayona, P Baddam and D Graf. Craniofacial development: Neural crest in molecular embryology. *Head Neck Pathol*. 2021; **15**, 1-15.

[4] Y Chai and RE Maxson Jr. Recent advances in craniofacial morphogenesis. *Dev. Dynam.* 2006; **235**, 2353-75.

[5] HN Shah, RE Jones, MR Borrelli, K Robertson, A Salhotra, DC Wan and MT Longaker. Craniofacial and long bone development in the context of distraction osteogenesis. *Plast. Reconstr. Surg*. 2021; **147**, 54e-65e.

[6] R Tevlin, A McArdle, D Atashroo, GG Walmsley, K Senarath-Yapa, ER Zielins, KJ Paik, MT Longaker and DC Wan. Biomaterials for craniofacial bone engineering. *J. Dent. Res*. 2014; **93**, 1187-95.

[7] SRF Twigg and AOM Wilkie. New insights into craniofacial malformations. *Hum. Mol. Genet.* 2015; **24**, R50-R59.

[8] ER Tamm. *The development of the aqueous humor outflow pathway*. *In*: DA Dartt (Ed.). Encyclopedia of the eye. Academic Press, Massachusetts, 2010, p. 16-21.

[9] M Helwany, TC Arbor and P Tadi. *Embryology, ear.* StatPearls Publishing, Treasure Island, Florida, 2020.

[10] TM Farhan, BA Al-Abdely, AN Abdullateef and AS Jubair. Craniofacial anomaly association with the internal malformations in the pediatric age group in Al-Fallujah City-Iraq. *Biomed. Res. Int*. 2020; **2020**, 4725141.

[11] W Shaw. Global strategies to reduce the health care burden of craniofacial anomalies: Report of WHO meetings on international collaborative research on craniofacial anomalies. *Cleft Palate Craniofac. J.* 2004; **41**, 238-43.

[12] S Liu, R Narumi, N Ikeda, O Morita and J Tasaki. Chemical-induced craniofacial anomalies caused by disruption of neural crest cell development in a zebrafish model. *Dev. Dyn*. 2020; **249**, 794-815.

[13] W Huang, T Wu, WW Au and K Wu. Impact of environmental chemicals on craniofacial skeletal development: Insights from investigations using zebrafish embryos. *Environ. Pollut*. 2021; **286**, 117541.

[14] ME Bronner and NM LeDouarin. Development and evolution of the neural crest: An overview. *Dev. Biol*. 2012; **366**, 2-9.

[15] BK Hall. *The neural crest and neural crest cells in vertebrate development and evolution*. Springer, New York, 2008, p. 400.

[16] J Casale and AO Giwa. *Embryology, branchial arches.* StatPearls Publishing, Treasure Island, Florida, 2021.

[17] R Hunt and PN Hunt. The role of cell mixing in branchial arch development. *Mech. Dev* 2003; **120**, 769-90.

[18] P Noisa and T Raivio. Neural crest cells: From developmental biology to clinical interventions. *Birth Defects Res. Part C Embryo Today* 2014; **102**, 263-74.

[19] TL Creazzo, RE Godt, L Leatherbury, SJ Conway and ML Kirby. Role of cardiac neural crest cells in cardiovascular development. *Annu. Rev. Physiol*. 1998; **60**, 267-86.

[20] MN Vergara and MV Canto-Soler. Rediscovering the chick embryo as a model to study retinal development. *Neural Dev.* 2012; **7**, 22.

[21] MR Passos-Bueno, CC Ornelas and RD Fanganiello. Syndromes of the first and second pharyngeal arches: A review. *Am. J. Med. Genet. Part A* 2009; **149**, 1853-9.

[22] JM Johnson, G Moonis, GE Green, R Carmody and HN Burbank. Syndromes of the first and second branchial arches, part 1: Embryology and characteristic defects. *Am. J. Neuroradiol*. 2011; **32**, 14-9.

[23] SA Green, M Simoes-Costa and ME Bronner. Evolution of vertebrates as viewed from the crest. *Nature* 2015; **520**, 474-82.

[24] MED Bellard, Y Rao and M Bronner-Fraser. Dual function of Slit2 in repulsion and enhanced migration of trunk, but not vagal, neural crest cells. *Int. J. Cell Biol*. 2003; **162**, 269-79.

[25] Y Shi, J Li, C Chen, M Gong, Y Chen, Y Liu, Jie Chen, Tingyu Li and W Song. 5-Mehtyltetrahydrofolate rescues alcohol-induced neural crest cell migration abnormalities. *Mol. Brain* 2014; **7**, 67.

[26] S Cerrizuela, GA Vega-Lopez and MJ Aybar. The role of teratogens in neural crest development. *Birth Defects Res.* 2020; **112**, 584-632.

[27] KM Appaiah. *Monosodium glutamate in foods and its biological effects*. *In*: CE Boisrobertm, A Stjepanovic, S Oh and HLM Lelieveld (Eds.). Ensuring global food safety: Exploring Global Harmonization. Elsevier, Amsterdam, Netherlands, 2010, p. 217-26.

[28] K Beyreuther, HK Biesalski, JD Fernstrom, P Grimm, WP Hammes, U Heinemann, O Kempski, P Stehle, H Steinhart and R Walker. Consensus meeting: Monosodium glutamate - an update. *Eur. J. Clin. Nutr.* 2007; **61**, 304-13.

[29] Z Kazmi, I Fatima, S Perveen and SS Malik. Monosodium glutamate: Review on clinical reports. *Int. J. Food Prop*. 2017; **20**, 1807-15.

[30] K Niaz, E Zaplatic and J Spoor. Extensive use of monosodium glutamate: A threat to public health? *EXCLI J.* 2018; **17**, 273-8.

[31] J Roongruangchai, Y Viravud, V Plakornkul, K Sripaoraya, W Boonmark and K Roongruangchai. The teratogenic effects of monosodium glutamate (MSG) on the development of chick embryos. *Siriraj Med. J.* 2018; **70**, 514-22.

[32] F Al-Qudsi and A Al-Jahdali. Effect of monosodium glutamate on chick embryo development. *J. Am. Sci*. 2012; **8**, 499-509.

[33] A Zanfirescu, A Ungurianu, AM Tsatsakis, GM Nițulescu, D Kouretas, A Veskoukis, D Tsoukalas, AB Engin, M Aschner and D Marginã. A review of the alleged health hazards of monosodium glutamate. *Compr. Rev. Food Sci. Food Saf*. 2019; **18**, 1111-34.

[34] S Pintarasri, V Plakornkul, Y Viravud, W Payuhakrit and T Rungruang. Folic acid attenuates MSG-induced teratogenicity during A 2-month pregnancy by preventing neural crest cell destruction and malformation in chick embryo models. *Trends Sci.* 2023; **20**, 6656-6.

[35] E Fauzia, TK Barbhuyan, AK Shrivastava, M Kumar, P Garg, MA Khan, AAB Robertson and SS Raza. Chick embryo: A preclinical model for understanding ischemia-reperfusion mechanism. *Front. Pharmacol*. 2018; **9**, 1034.

[36] M Fisher and CG Schoenwolf. The use of early chick embryos in experimental embryology and teratology: Improvements in standard procedures. *Teratology* 1983; **27**, 65-72.

[37] J Männer, W Seidl, F Heinicke and H Hesse. Teratogenic effects of suramin on the chick embryo. *Anat. Embryol*. 2003; **206**, 229-37.

[38] GK Uggini, PV Patel and S Balakrishnan. Embryotoxic and teratogenic effects of pesticides in chick embryos: A comparative study using two commercial formulations. *Environ. Toxicol*. 2012; **27**, 166-74.

[39] H Butler and BH Juurlink. *An atlas for staging mammalian and chick embryos*. CRC Press, Florida, 2018, p. 232.

[40] B Arnaout, KE Lantigua, EM MacKenzie, IW McKinnell and HC Maddin. Development of the chicken skull: A complement to the external staging table of Hamburger and Hamilton. *Anat. Rec.* 2021; **304**, 2726-40.

[41] FAM Al-Ghamdi. Pomegranate peel extracts effects to reduce monosodium glutamate toxic effects on chicken embryos: Morphological studies. *Saudi J. Biol. Sci*. 2022; **29**, 975-83.

[42] G Breeland, MA Sinkler and RG Menezes. *Embryology, bone ossification.* StatPearls Publishing, Treasure Island, Florida, 2023.

[43] P Zhang, G Wang, Z Lin, Y Wu, J Zhang, M Liu, KKH Lee, M Chuai and X Yang. Alcohol exposure induces chick craniofacial bone defects by negatively affecting cranial neural crest development. *Toxicol. Lett*. 2017; **281**, 53-64.

[44] A Adams, K Mankad, C Offiah and L Childs. Branchial cleft anomalies: A pictorial review of embryological development and spectrum of imaging findings. *Insights Imaging*. 2016; **7**, 69-76.

[45] MS Demirtaş. *The pathogenesis of congenital anomalies: Roles of teratogens and infections*. *In:* RP Verma (Ed.). Congenital anomalies in newborn infants-clinical and etiopathological perspectives. IntechOpen, London, 2020, p. 226.

[46] P Zhang, G Wang, Z Lin, Y Wu, J Zhang, M Liu, KKH Lee, M Chuai and X Yang. Alcohol exposure induces chick craniofacial bone defects by negatively affecting cranial neural crest development. *Toxicol. Lett.* 2017; **281**, 53-64.

[47] KN Thomas, N Srikanth, SS Bhadsavle, KR Thomas, KN Zimmel, A Basel, AN Roach, NA Mehta, YS Bedi and MC Golding. Preconception paternal ethanol exposures induce alcohol-related craniofacial growth deficiencies in fetal offspring. *J. Clin. Invest.* 2023; **133**, e167624.

[48] C Therapontos, L Erskine, ER Gardner, WD Figg and N Vargesson. Thalidomide induces limb defects by preventing angiogenic outgrowth during early limb formation. *Proc. Natl. Acad. Sci. U. S. A*. 2009; **106**, 8573-8.

[49] JH Kim and AR Scialli. Thalidomide: The tragedy of birth defects and the effective treatment of disease. *Toxicol. Sci.* 2011; **122**, 1-6.

[50] DA Ridenour, R McLennan, JM Teddy, CL Semerad, JS Haug and PM Kulesa. The neural crest cell cycle is related to phases of migration in the head. *Development* 2014; **141**, 1095-103.

[51] Y Yan, G Wang, J Huang, Y Zhang, X Cheng, M Chuai, B Brand-Saberi, G Chen, X Jiang and X Yang. Zinc oxide nanoparticles exposure-induced oxidative stress restricts cranial neural crest development during chicken embryogenesis. *Ecotoxicol. Environ. Saf*. 2020; **194**, 110415.